

## 5. Conclusions

The above calculations provide a quantitative test of the mechanism of disordering in stilbene which has been suggested by X-ray data. The results confirm that the proposed model of orientational disordering is quite plausible and may be responsible for the apparent shortening of the central  $-C=C-$  bond. All the atomic displacements due to the disorder, save those for the central C atoms, can apparently be accommodated by anisotropic temperature factors. As a result of the rectangular arrangement of the ordered and disordered central atoms, which places them all at least  $\sim 1 \text{ \AA}$  apart, the refinement tends to 'concentrate' the electron density towards the centre of the molecule, leading to an apparent shortening of the bond. It does not appear that other satisfactory models of orientational disordering in *trans*-stilbene can differ significantly from the one presented here.

The atom-atom potential method has been shown to be very convenient and useful for testing models for disordering in molecular crystals. The method is sensitive to small changes in crystal structure and yields results consistent with the crystallographic structural studies.

The calculation procedure, described here, appears to be quite general and should be applicable to any molecular crystal with orientational disorder.

The authors thank Professor M. D. Cohen for his interest in the work and a helpful discussion of the manuscript.

## References

- BERNSTEIN, J. (1975). *Acta Cryst.* **B31**, 1268–1271.  
 BERNSTEIN, J., BAR, I. & CHRISTENSEN, A. (1976). *Acta Cryst.* **B32**, 1609–1611.  
 BROWN, C. J. (1966a). *Acta Cryst.* **21**, 153–158.  
 BROWN, C. J. (1966b). *Acta Cryst.* **21**, 146–152.  
 FINDER, C. J., NEWTON, M. G. & ALLINGER, N. L. (1974). *Acta Cryst.* **B30**, 411–415.  
 FRANK, G. W., MYASNIKOVA, R. M. & KITAIGORODSKII, A. I. (1971). *Sov. Phys. Crystallogr.* **16**, 270–274.  
 HOEKSTRA, A., MEERTENS, P. & VOS, A. (1975). *Acta Cryst.* **B31**, 2813–2817.  
*International Tables for X-ray Crystallography* (1962). Vol. II. Birmingham: Kynoch Press.  
 KITAIGORODSKY, A. I. (1973). *Molecular Crystals and Molecules*. New York: Academic Press.  
 MIRSKAYA, K. V., KOZLOVA, I. E. & BEREZNIITSKAYA, V. F. (1974). *Phys. Status Solidi B*, **62**, 291–294.  
 MIRSKY, K. (1976). *Acta Cryst.* **A32**, 199–207.  
 MORAWETZ, E. (1972). *J. Chem. Thermodyn.* **4**, 455–460.  
 REYNOLDS, P. A. (1975). *Acta Cryst.* **A31**, 80–83.  
 ROBERTSON, J. M. & WOODWARD, I. (1937). *Proc. R. Soc. London*, **A162**, 568–583.  
 SAMARSKAYA, V. D., MYASNIKOVA, R. M. & KITAIGORODSKII, A. I. (1969). *Sov. Phys. Crystallogr.* **13**, 525–529.  
 WILLIAMS, D. E. (1972). *Acta Cryst.* **A28**, 629–635.

*Acta Cryst.* (1978). **A34**, 165–170

## Analysis of Polytypic Structure with Stacking Faults on the Basis of X-ray Powder Patterns

BY B. PAŁOSZ AND J. PRZEDMOJSKI

*Institute of Physics, Warsaw Technical University, 00-662 Warszawa, ul. Koszykowa 75, Poland*

(Received 16 May 1977; accepted 2 August 1977)

In this paper the possibility of applying powder diffraction patterns to determine polytypes and stacking sequences in disordered close-packed structures is discussed. It is shown that by using model structure analysis it is possible to establish some important features of the structure such as the presence of DS (Disordered Structure) and various simple polytypes.

## Introduction

Polytypic structures with stacking faults are usually investigated on the basis of X-ray patterns obtained by the oscillating crystal method: Singer (1963), Ebina & Takahashi (1967), Farkas-Jahnke & Dornberger-Schiff (1970), Pałosz & Przedmojski (1976a,b). In earlier papers (Pałosz & Przedmojski, 1976a,b; Pałosz, B.,

1977) an application of a structural-model method to the analysis of crystals with stacking faults was discussed. In that method the structure determination was based on the comparison of (1) experimental intensity curves, obtained by photometering of  $10.L$  reflexions from oscillating crystal patterns, with (2) calculated theoretical curves. The theoretical curves were obtained on the basis of computed intensities for the  $10.L$  re-

flexions from a series of hypothetical structure models. The detailed description of the method of calculating theoretical curves was presented in our earlier paper (Pałosz & Przedmojski, 1976*b*). The distribution curves are drawn as a function of coordinates  $I = f(L/m)$ , where  $m$  is the number of layers in a given polytype cell. This method has been successfully applied to the investigation of ZnS and ZnS solid solutions (Pałosz, B., 1977).

In practice it is often necessary to analyse the polytypic structure of polycrystalline materials. There are many papers concerned with this subject, in which the main problem in structure analysis is the determination of probability parameters for the appearance of respective layer sequences (Warren, 1959; Sato, 1969; Farkas-Jahnke, 1973*a,b*; etc.). In this paper the possibility of applying the model method to analysis of X-ray powder patterns is discussed. This analysis is limited to comparison of experimental curves obtained from X-ray patterns of the crystal oscillating around the  $c$  axis with diffraction patterns obtained for powders of the same crystals of ZnS and its solid solution. The diffraction patterns were examined in the angle range  $26^\circ < 2\theta < 34^\circ$ , i.e. the range in which the  $10.L$  reflexions appear. These comparisons and knowledge of the positions and intensities of reflexions appearing in both intensity distributions permit the establishment of a correlation between the influences of stacking faults on the shape of intensity curves obtained for polycrystals and monocrystals, and from there the determination of approximate information concerning the stacking sequence in the crystal.

### Experimental conditions

Diffraction patterns of powdered crystals were obtained with Cu  $K$  radiation monochromatized with the aid of a flat plate of LiF. The URS-50 IM diffractometer with scintillation counter and automatic registration of the diffraction patterns was used, at  $\frac{1}{4}^\circ/\text{min}$  counter rotation speed and 1 cm/min tape feed speed. The parameters of the primary beam were 9 mA and 36 kV. Slits of 0.5 mm were used. All diffraction patterns were obtained under the same experimental conditions.

The single-crystal intensity distribution curves were obtained by photometering the  $10.L$  reflexion line in the  $c^*$  direction from X-ray patterns of a crystal oscillating about  $c$  in a  $15^\circ$  range with a camera of 86 mm internal diameter and a collimator of aperture  $\frac{1}{2}$  mm. The size of the focal spots was about  $1 \text{ mm}^2$ . The crystals were 1–2 mm in length and about 0.5 mm in diameter. In this case, a nickel  $\beta$ -filter was used with the Cu  $K$  radiation.

The oscillation photographs about  $c$  were taken over a  $15^\circ$  range between the positions where the  $a$  axis made angles of  $10.5^\circ$  and  $25.5^\circ$  with the incident X-ray beam. This range of oscillation is the most

suitable as it records the  $10.L$  row for  $-0.8 \lesssim L/m \lesssim 0.8$  for any zinc sulphide structure. The intensity measurements were made with the help of a recording-type microphotometer. For determination of intensities from photometric traces, a standard calibration curve of photographic density of blackening *versus* exposure time was drawn. The curve thus obtained was used to read the intensity values.

### Results

Figs. 1 and 2 show diffraction patterns from ZnS crystals obtained by the chemical transport method (Pałosz, W., 1978) for the  $2H$  and  $3C$  structures without stacking faults. The comparison of powder diffraction patterns (a) with the intensity curves obtained by the oscillating-crystal method (b) for ZnS solid-solution crystals obtained by the Bridgman method (Koziełski, 1975) is presented in Figs 3–8. The

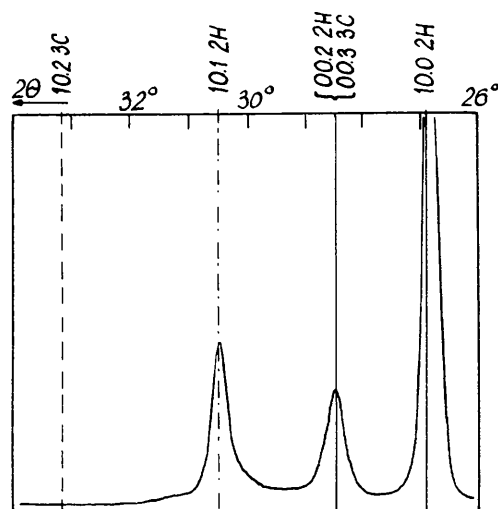


Fig. 1. Powder pattern for crystal of  $2H$  structure.

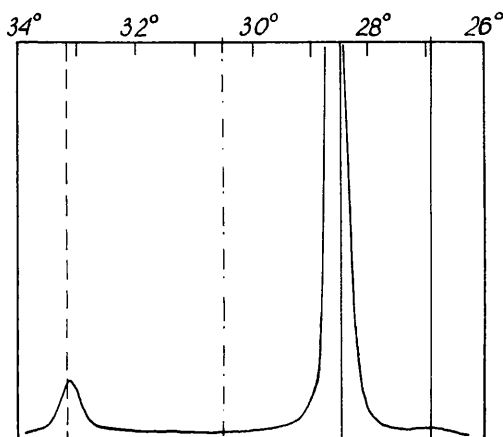


Fig. 2. Powder pattern for crystal of  $3C$  structure.

curves in Fig. 3 correspond to crystals with  $2H$  (10%) +  $4H$  (60%) +  $6H$  (30%) structure with monopolytype fragments equal on average to two  $2H$  cells, four  $4H$  cells and two  $6H$  cells. In the crystal structure the occurrence of DS fragments occupying less than 5–10% of the total number of layers, *i.e.* less than the sensitivity of the model method, is possible. (DS is described as a lack of any periodicity in the arrangement of layer sequences – Pałosz, B., 1977). In Fig. 3(a) one may clearly discern the reflexions from the different polytypes:  $2H$ –10.0 (maximum 1) and 10.1 (7),  $4H$ –10.0 (1), 10.1 (3) and 10.2 (7) as well as  $6H$ –10.1 (2) and 10.3 (7). The number in parentheses represents the peak position in the diffraction pattern. It is characteristic that, while the maximum of the curve in (b) corresponds to the reflexion in position  $L/m = 0.5$ , the maximum in (a) corresponds to the position  $L/m = 0.25$ . This is the result of the addition of the integrated intensity of maxima appearing in the range of angle close to the position  $L/m = 0.25$  and a simultaneous ‘stretching’ of the integrated intensity of the maximum at  $L/m = 0.5$  over a wider range of  $2\theta$

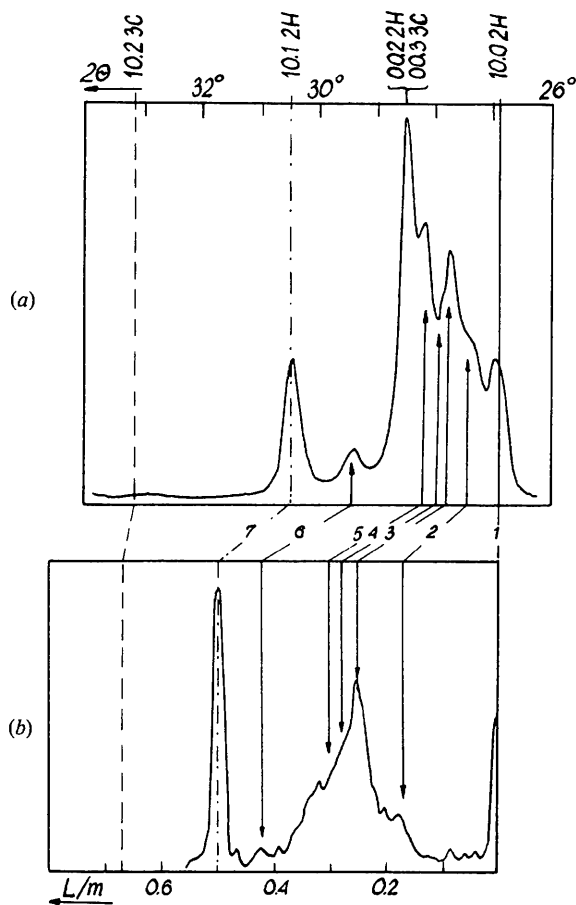


Fig. 3. Intensity curves for structure  $2H$  (10%) +  $4H$  (60%) +  $6H$  (30%). Monopolytype fragments are of two  $2H$  cells, four  $4H$  cells and two  $6H$  cells.

angles. In this case we take into consideration only characteristic reflexions, *i.e.*  $10.L$ , neglecting reflexions  $00.m$ , *e.g.*  $00.2$  for  $2H$  and  $00.3$  for  $3C$ .

Fig. 4 shows intensity curves obtained for crystals of  $6H$  (40%) + DS (30–35%) structure with 1–2  $6H$  cells in the fragments. In (a) and (b) one can see reflexions from  $6H$  with, however, as in Fig. 3, significant changes in the intensity ratios of particular reflexions. The minima of intensity, between maxima 4 and 5, 7 and 8 and 10 and 11, are also characteristic of the curves. Reflexion 10.2 of  $6H$  ( $L/m = 0.33$ ,  $2\theta = 28.6^\circ$ ) does not appear as a separate maximum in (a), because for  $2\theta = 28.5^\circ$  the much stronger reflexion  $00.6$  of polytype  $6H$  appears.

Intensity curves corresponding to crystal structure  $6H$  (10%) +  $10H$  (30%) + DS (30%) with fragments composed on the average of two  $6H$  cells and two  $10H$  cells are shown in Fig. 5. In (b) one can distinguish broadened  $10H$  reflexions (10.2, 10.3, 10.4, 10.6 and 10.7), whereas in (a) the corresponding reflexions are only just detectable; 10.2 (maxima 3 and 4), 10.3 (6), 10.4 (8). Reflexion 10.3 of  $6H$  (maximum 11) is also visible on both curves. It is necessary to note that in (a)

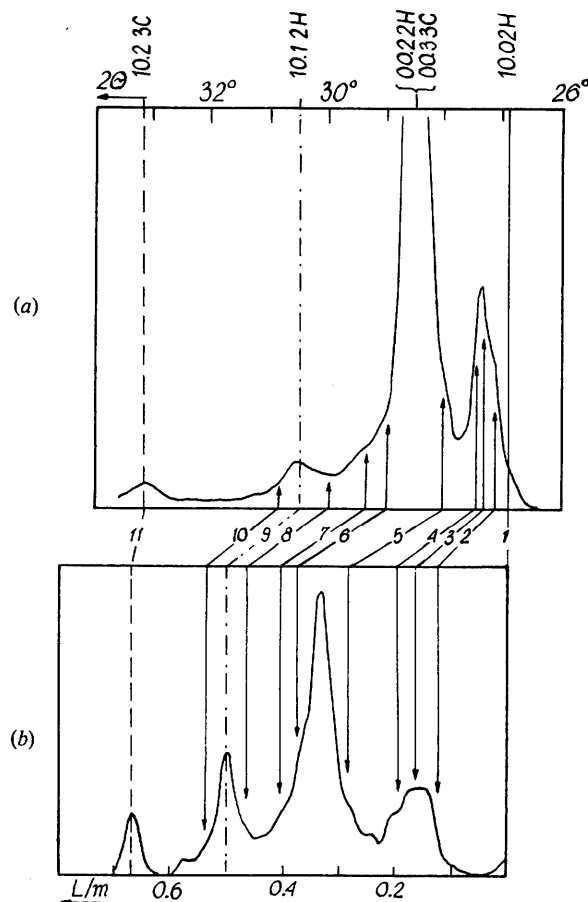


Fig. 4. Intensity curves for  $6H$  (40%) + DS (30–35%) structure with 1–2  $6H$  cells in the fragments.

there appears a strong maximum (1) reflexion  $10.0$  of  $2H$  or  $10.0$  of  $4H$ , which is not present in (b).

Figs. 6, 7, 8 were obtained for similar structures of the type  $2H + DS$ , differing significantly, however, in the sizes of fragments composed of  $2H$  cells appearing one after another.

Fig. 6 presents results for the structure  $2H$  (20%) + DS (50%) which contains 1–2  $2H$  cells in the fragments. In (b) the integral intensity is mainly contained in two maxima: (1)  $L/m$  from 0.0 to 0.2 and (2)  $L/m$  from 0.35 to 0.55. In (a) the first sharp maximum appears for  $2\theta = 27^\circ$ , while the second maximum is stretched over the approximate range from  $2\theta = 28^\circ$  to  $2\theta = 31^\circ$ , where one may discern weakly marked maxima 7–12, characteristic of DS.

In contrast to Fig. 6 one can see in Fig. 7 several clearly marked maxima. For this reason the intensity in (a) is concentrated in several clearly distinguishable maxima: (1), (4), (7), (9) and (10). The appearance of sharp maximum (7) from DS is characteristic.

Intensity distribution curves for structure  $2H$  (20%) + DS (50%) with 10  $2H$  cells in the fragments are

shown in Fig. 8. All the maxima appearing in (a) are repeated in (b).

Thus in spite of the similarity between the structures giving rise to the patterns of Figs. 6–8, significant differences in intensity distribution are observed between the curves in both (a) and (b). Curves in (a) and (b) in each particular figure, however, exhibit a good correlation.

### Summary

1. On the whole, a close relation was noted between corresponding intensity curves obtained from mono- and polycrystals. From the comparison of experimental results presented for ZnS and its solid solutions it follows that it is possible to employ theoretical curves obtained on the basis of structural models for the interpretation of intensity profiles obtained by the powder method. A comparison of the two types of intensity curve is facilitated by Table 1. As is evident from the table, only one reflexion other than  $10.L$  appears for polytypes  $2H$ ,  $3C$ ,  $4H$ ,  $6H$  and  $10H$  in the

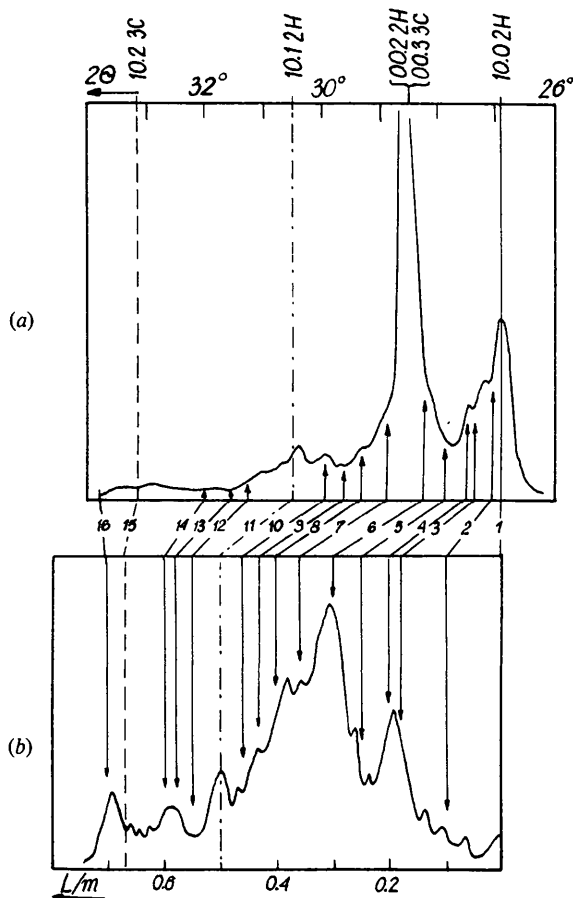


Fig. 5. Intensity curves for  $6H$  (20%) +  $10H$  (30%) + DS (30%) structure with 2–3  $6H$  cells and 2  $10H$  cells in the fragments.

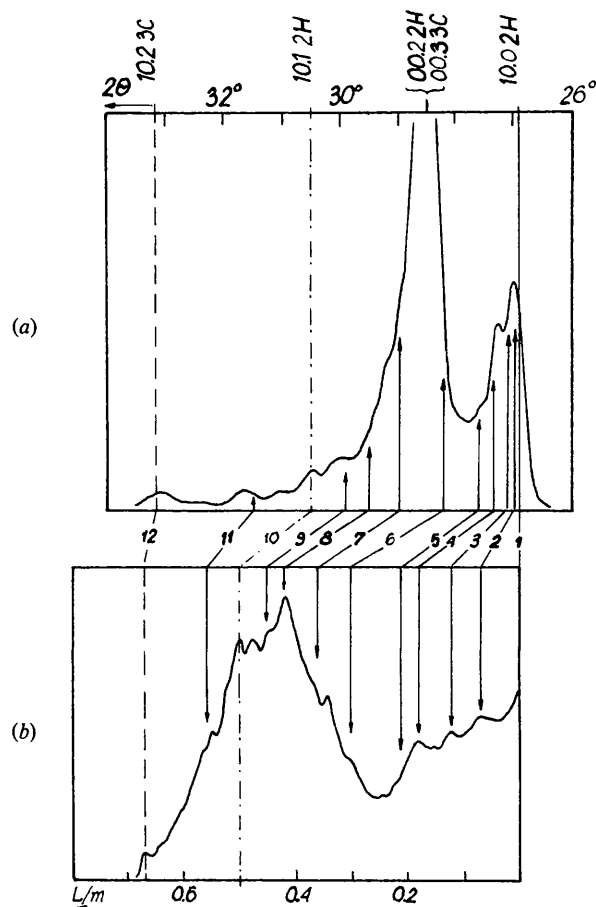


Fig. 6. Intensity curves for  $2H$  (15–25%) + DS (50%) with 1–3  $2H$  cells in the fragments.

investigated range of  $2\theta$  angles. This is reflexion  $00.m$ , the position of which is independent of the structure layer sequence. The appearance of respective polytypes may be confirmed by the presence of reflexions that do not coincide with reflexion  $00.m$  or with reflexions of the remaining polytypes; for example: (a) the appearance of polytype  $3C$  in the presence of  $2H$  can be determined on the basis of reflexion  $10.2$  for  $L/m = 0.67$  ( $2\theta = 33.15^\circ$ ), (b) the presence of  $4H$  cells next to  $2H$  cells in the structure is proved by the appearance of reflexion  $10.1$  for  $L/m = 0.25$  ( $2\theta = 27.65^\circ$ ) together with a reflexion in position  $L/m = 0.0$  ( $2\theta = 26.95^\circ$ ), (c) the simultaneous appearance of reflexions  $10.1$  for  $L/m = 0.167$  ( $2\theta = 27.33^\circ$ ) and  $10.4$  for  $L/m = 0.67$  ( $2\theta = 33.15^\circ$ ) is characteristic of  $6H$  and permits the detection of the presence of  $6H$  next to  $2H$ ,  $3C$  and  $4H$ . Similar characteristic elements of the intensity profile may be discerned for other polytype pairs.

As the number of layers in a polytype cell increases, precise analysis of the appearance of particular polytypes becomes increasingly difficult. In particular, in intensity profiles obtained from powders one may

observe intensity maxima characterizing DS structure which may coincide with the positions of polytype reflexions, thus seriously complicating analysis of these reflexions.

2. Agreement between corresponding curves in (a) and (b) depends upon several factors: (i) In Fig. 5, for example, the differences between (a) and (b) may be connected with structure inhomogeneity. In the powder method large amounts of crystal are used compared with the amount in the single-crystal oscillating method. Therefore the appearance in (a) of the maximum corresponding to reflexion  $10.0$  of  $2H$  may be the result of a coincidental appearance of  $2H$  cells in a dominantly  $6H + 10H + DS$  structure. (ii) Overlapping of broadened reflexions: in the investigated range of  $L/m$  values;  $10.L$  reflexions with neighbouring  $L$  values lie at approximately the same distance from each other on the oscillation photograph both for  $L/m = 0$  and for  $L/m = 1$ . In the powder pattern, however, the distance between neighbouring reflexions changes according to the  $2\theta$  angle, and the broadening of adjacent reflexions has an essential influence on the shape of the intensity

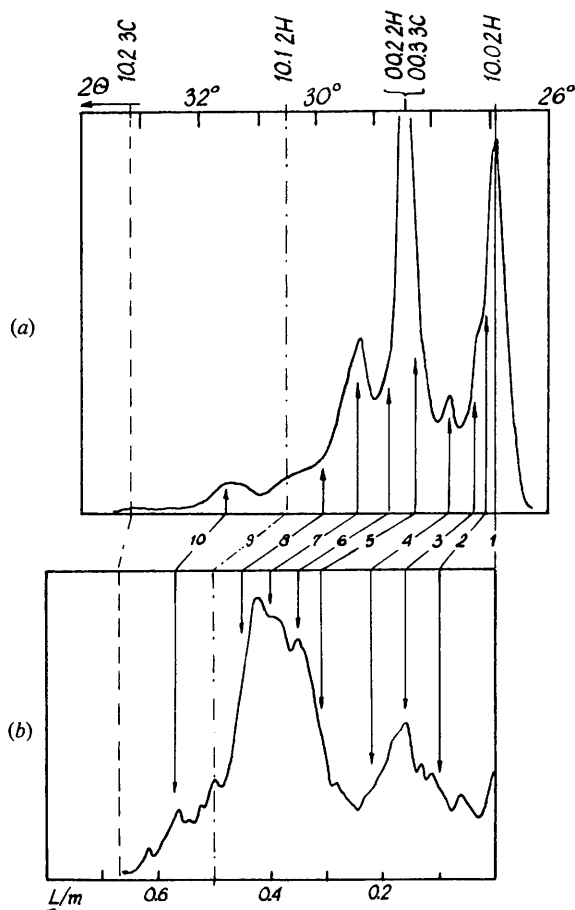


Fig. 7. Intensity curves for  $2H$  (20%) + DS (35–50%h) structure with about 2  $2H$  cells in the fragments.

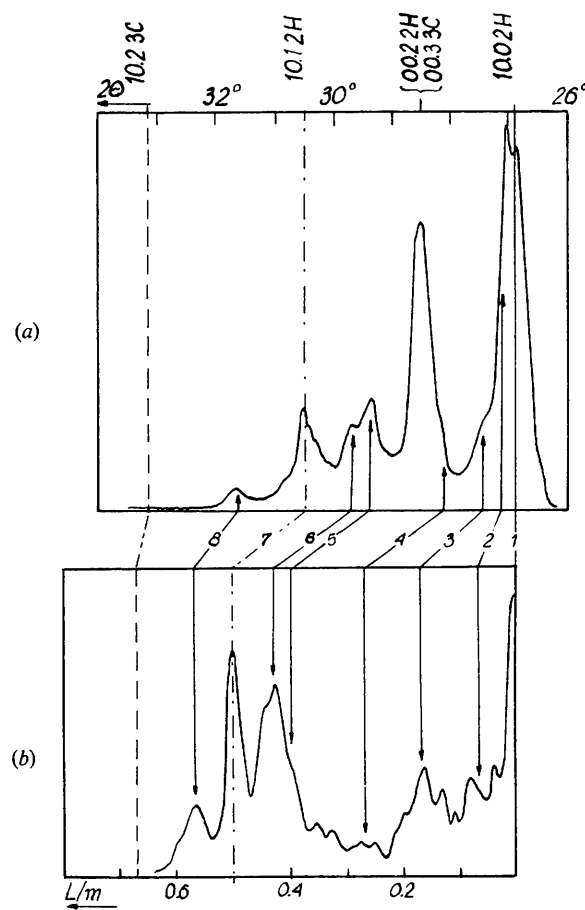


Fig. 8. Intensity curves for  $2H$  (20%) + DS (50%h) structure with about 10  $2H$  cells in the fragments.

Table 1. *Reflexions observed for simple polytypes*

	No.	Oscillation photograph			Powder pattern			
		<i>HK.L</i>	<i>L/m</i>	<i>I<sub>calc</sub></i>	<i>d</i>	<i>2θ</i>	<i>I<sub>calc</sub></i>	<i>I<sub>obs</sub></i>
2 <i>H</i>	1	10.0	0.0	100	3.31	26.95	100	100
	2	00.2	—	—	3.13	28.50	62	20
	3	10.1	0.50	52	2.92	30.50	92	30
3 <i>C</i>	1	00.3	—	—	3.13	28.50	100	100
	2	10.1	0.33	100	3.12	28.60	0	0
	3	10.2	0.67	13	2.70	33.15	64	10
4 <i>H</i>	1	10.0	0.0	50	3.31	26.95	26	
	2	10.1	0.25	100	3.20	27.85	100	
	3	00.4	—	—	3.13	28.50	62	
	4	10.2	0.50	78	2.92	30.50	71	
6 <i>H</i>	1	10.1	0.167	58	3.26	27.33	60	
	2	00.6	—	—	3.13	28.50	67	
	3	10.2	0.33	100	3.12	28.60	100	
	4	10.3	0.50	48	2.92	30.50	45	
	5	10.4	0.667	12	2.70	33.15	11	
10 <i>H</i>	1	10.0	0.0	9	3.31	26.95	5	
	2	10.1	0.1	4	3.29	27.10	3	
	3	10.2	0.2	23	3.24	27.50	24	
	4	10.3	0.3	100	3.15	28.25	100	
	5	00.10	—	—	3.13	28.50	70	
	6	10.4	0.4	70	3.05	29.33	68	
	7	10.5	0.5	5	2.92	30.50	4	
	8	10.6	0.6	16	2.79	32.00	14	
	9	10.7	0.7	11	2.66	33.70	9	

profile. For example, the *L/m* range from 0.0 to 0.2 ( $\Delta L/m = 0.2$ ) corresponds to  $2\theta$  angles ranging from  $27^\circ$  to  $27.5^\circ$  ( $\Delta 2\theta = 0.5$ ), while the equivalent interval *L/m* in the range 0.4 to 0.6 corresponds to a  $2\theta$  angle range of  $29^\circ$  to  $32^\circ$  which gives  $\Delta 2\theta = 3^\circ$ . Resolution in the powder method is therefore a function of  $2\theta$  and is much better for maxima appearing at higher angles. Fig. 8(a) may serve as an example of good maxima separation.

3. The powder method makes possible the determination of the presence of DS structure. The maxima observed in Fig. 7 – maxima (3), (7) and (10) and in Fig. 8 – maxima (3), (5), (6) and (8) may serve as examples.

4. The possibility of detecting structure with stacking faults on the basis of an analysis of the shape of the whole intensity curve seems particularly important for structures not near to 2*H* (h.c.p.) not to 3*C* (f.c.c.), where an intermediate phase between them has cells distinguished from other polytypes. For such structures intensity curves are characterized by a complex shape.

5. From the comparisons presented it follows that it is possible to apply a model method to the preliminary analysis of the structure of polycrystals. In curves in (b) one may observe essential details of the intensity

profiles, *i.e.* the asymmetry of the intensity distribution, clearly marked characteristic DS maxima *etc.*, while on corresponding curves in (a) many such details cannot be observed. Thus, although the powder method allows certain information to be obtained about the stacking sequences, this is less than can be derived from the investigation of monocrystals.

We thank Dr M. Kozielski and MSc W. Pałosz for supplying the crystals for the investigations.

#### References

- EBINA, A. & TAKAHASHI, T. (1967). *J. Appl. Phys.* **38**, 3079–3086.  
 FARKAS-JAHNKE, M. (1973a). *Acta Cryst.* **B29**, 407–413.  
 FARKAS-JAHNKE, M. (1973b). *Acta Cryst.* **B29**, 413–420.  
 FARKAS-JAHNKE, M. & DORNBERGER-SCHIFF, K. (1970). *Acta Cryst.* **A26**, 35–41.  
 KOZIELSKI, M. J. (1975). *J. Cryst. Growth*, **30**, 86–93.  
 PAŁOSZ, B. (1977). *Acta Cryst.* **A33**, 172–177.  
 PAŁOSZ, B. & PRZEDMOJSKI, J. (1976a). *Acta Cryst.* **A32**, 409–411.  
 PAŁOSZ, B. & PRZEDMOJSKI, J. (1976b). *Acta Cryst.* **A32**, 412–415.  
 PAŁOSZ, W. (1978). To be published.  
 SATO, R. (1969). *Acta Cryst.* **A25**, 309–318.  
 SINGER, J. (1963). *Acta Cryst.* **16**, 601–604.  
 WARREN, B. E. (1959). *Prog. Met. Phys.* **8**, 147–202.